Electronic Supplementary Material (ESI) for Dalton Transactions.

Supporting information

Precursor-mediated synthesis of $Cu_{2-x}Se$ nanoparticles and their composites with TiO_2 for improved photocatalysis

Sweta Gahlot,[a] Erwann Jeanneau,[b] Frederic Dappozze,[a] Chantal Guillard,[a] Shashank Mishra[a*]

[a] Université Lyon 1, CNRS, UMR 5256, IRCELYON, Institut de recherches sur la catalyse et l'environnement de Lyon, 2 avenue Albert Einstein, F-69626 Villeurbanne, France

[b] Université Lyon 1, Centre de Diffractométrie Henri Longchambon, 5 rue de La Doua, 69100 Villeurbanne, France

E-mail : shashank.mishra@ircelyon.univ-lyon1.fr; Fax: 33-472445399; Tel: 33 472445322.

a)

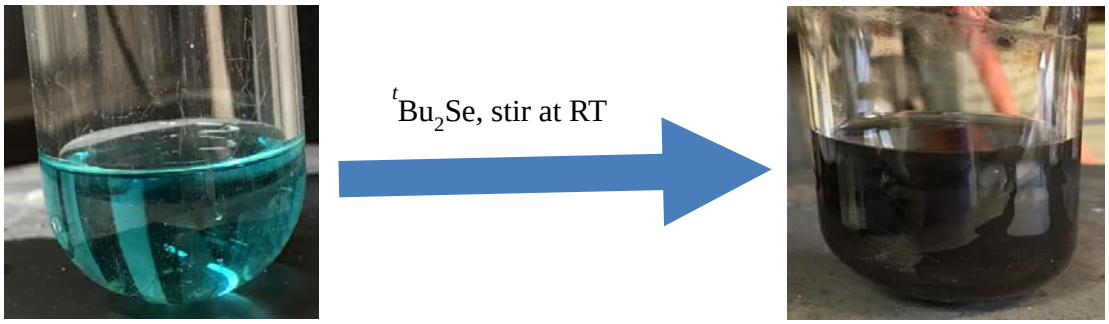

[Cu(TFA)$_2$] in Et$_2$O

Cu$_{2-x}$Se NPs

b)

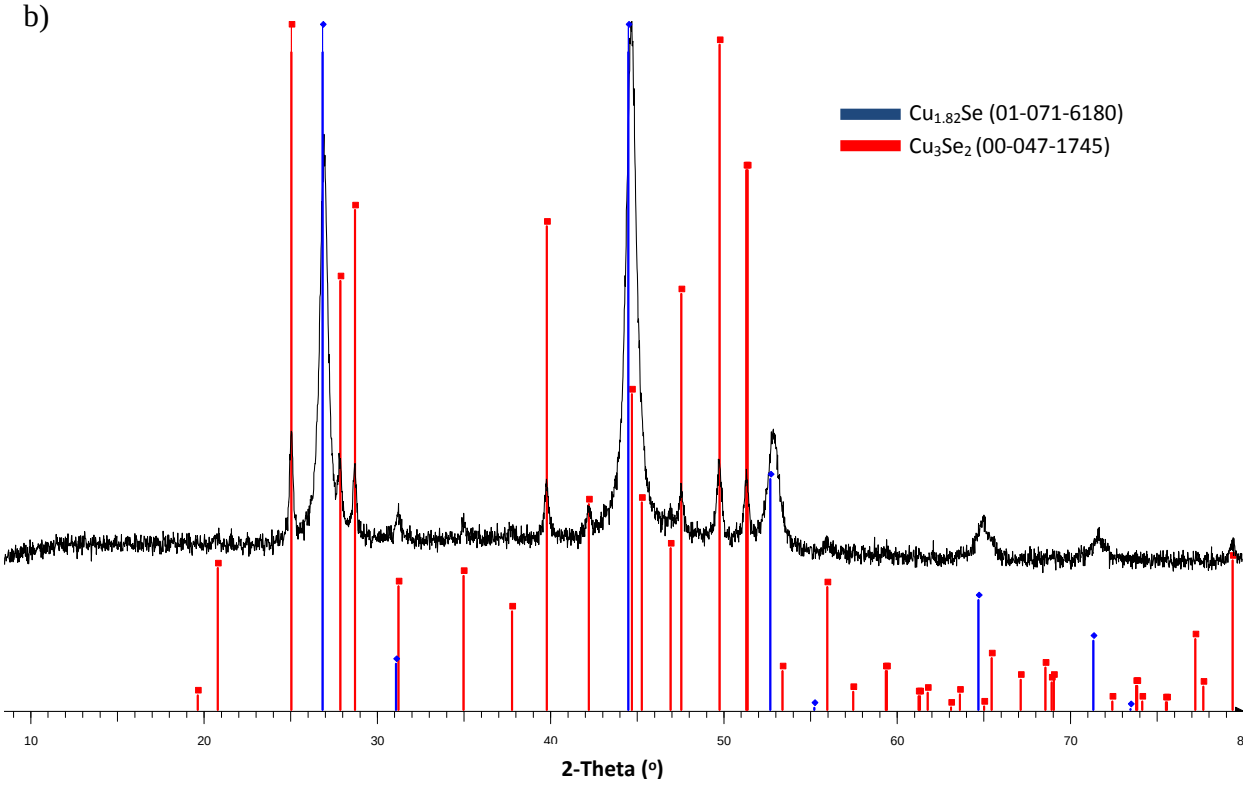

Figure S1. (a) Green coloured solution of Cu(TFA)$_2$ and ^{t}Bu$_2$Se in Et$_2$O on stirring at room temperature gradually turns black to give Cu$_{2-x}$Se NPs, and b) XRD pattern of the obtained Cu$_{2-x}$Se NPs.

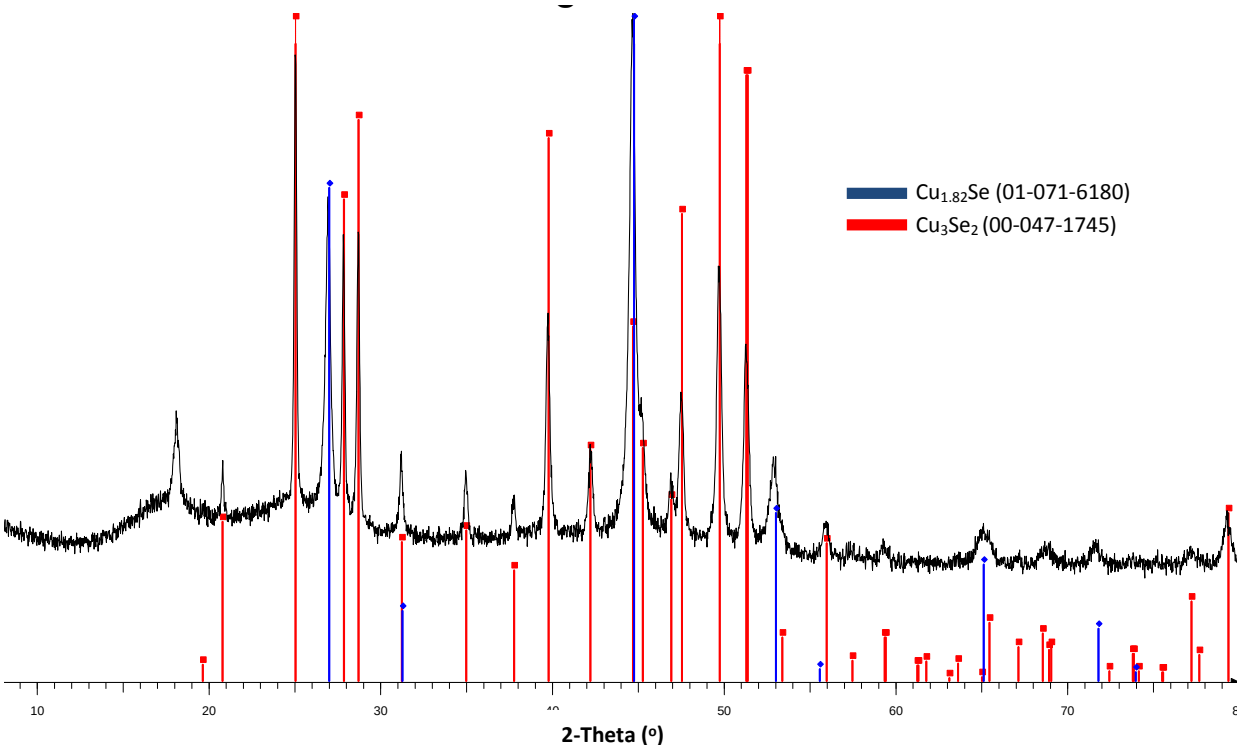

Figure S2. XRD pattern of $Cu_{1.82}Se$ and Cu_3Se_2 NPs obtained from the reaction of $Cu(TFA)_2$ and $^tBu_2Se$ after refluxing in THF at 65 °C for 3 h.

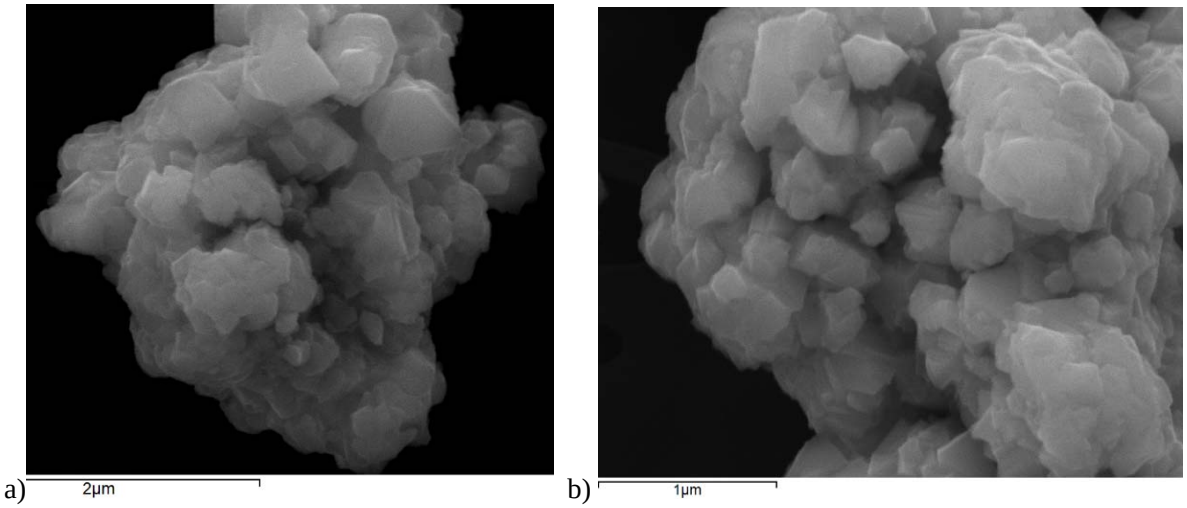

Figure S3. SEM images of $Cu_{2-x}Se$ NPs at different resolutions.

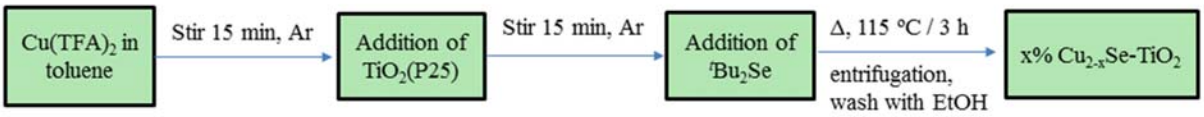

Figure S4. Schematic representation of the synthesis of the $Cu_{2-x}Se$-TiO_2 nanocomposites.

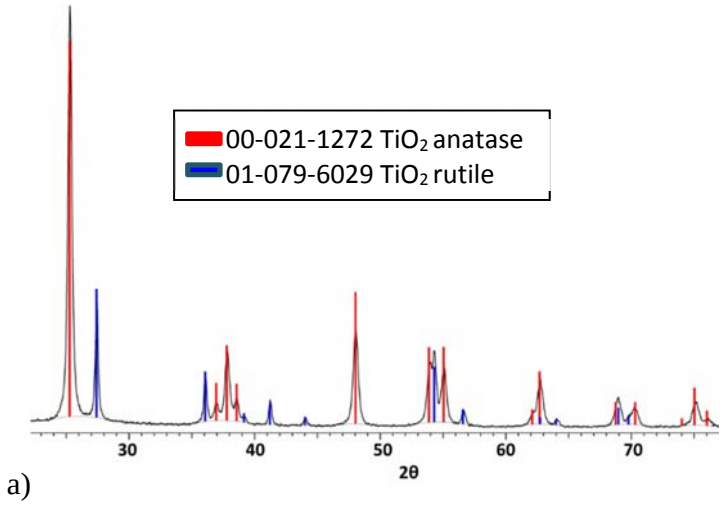

a)

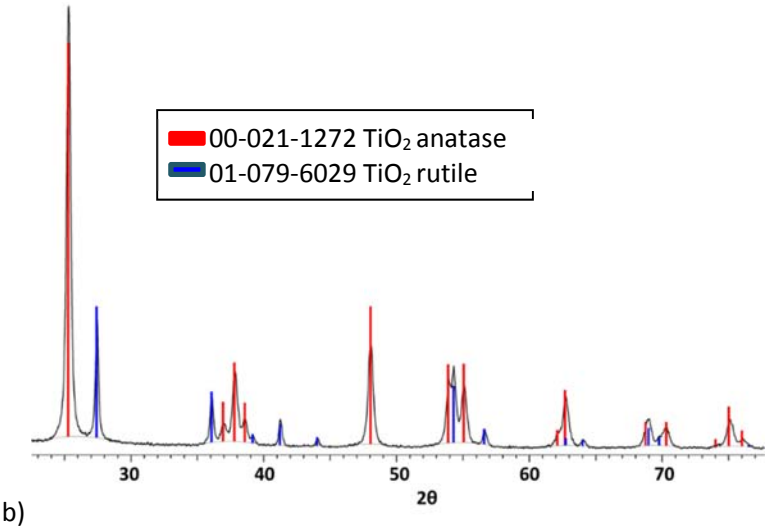

b)

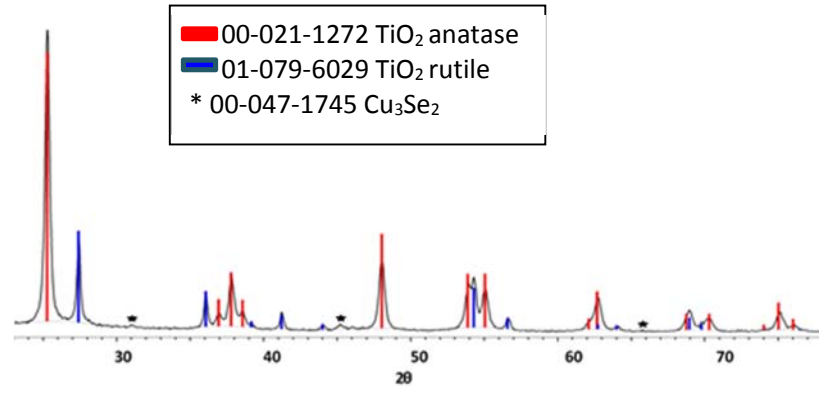

c)

Figure S5. XRD patterns of *n* mol% $Cu_{2-x}Se$-TiO_2 nanocomposites obtained from $Cu(TFA)_2$, $^tBu_2Se$ and TiO_2 under reflux in toluene at 115 °C for 3h. (a) 0.1% $Cu_{2-x}Se$-TiO_2, (b) 0.3% $Cu_{2-x}Se$-TiO_2 and (c) 1% $Cu_{2-x}Se$-TiO_2.

Table S1. BET surface area and related data of TiO_2 and $Cu_{2-x}Se$-TiO_2 nanocomposites

Sample Name	BET surface area (m^2/g)	Total pore volume (cm^3/g)	Av. pore diameter (nm)
TiO_2	58.9	0.23	15.6
0.1% $Cu_{2-x}Se$-TiO_2	52.8	0.33	25.0
0.3% $Cu_{2-x}Se$-TiO_2	47.9	0.28	23.5
1% $Cu_{2-x}Se$-TiO_2	51.0	0.22	17.7

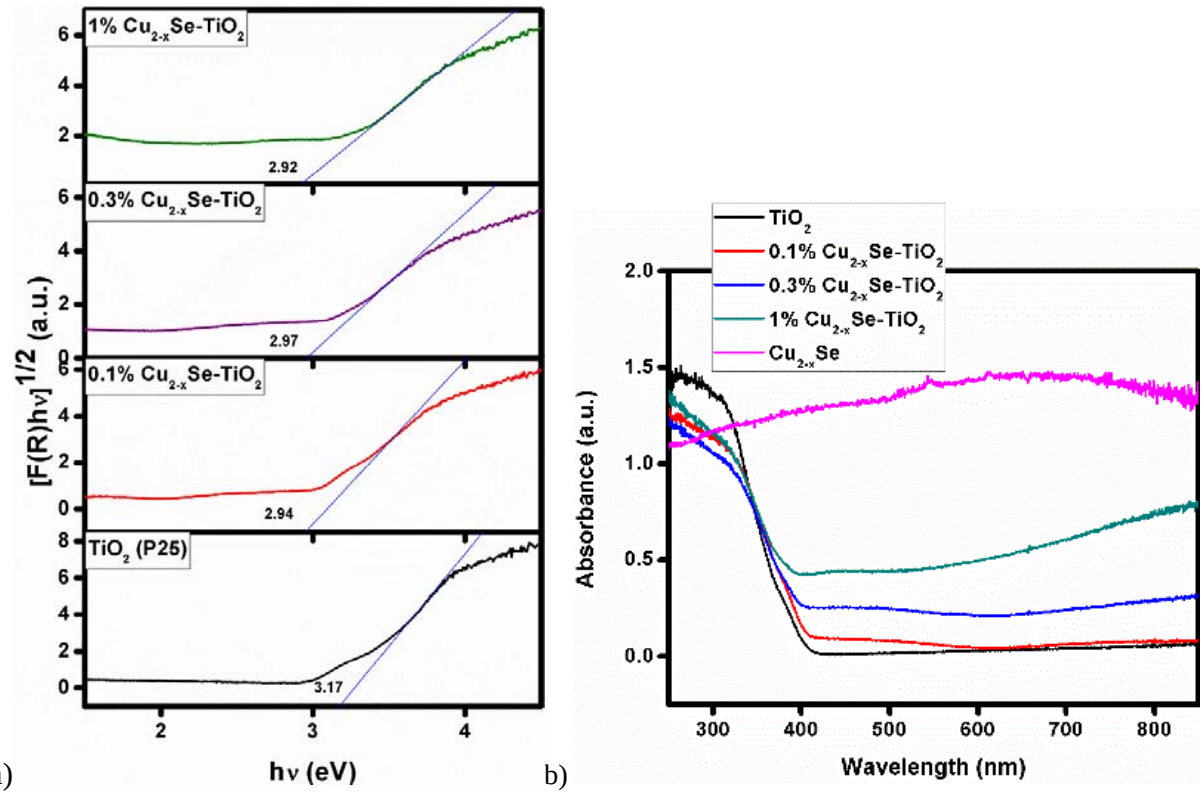

Figure S6. Kubelka munk plots (a) and UV-visible absorption spectra (b) of P25 and $Cu_{2-x}Se$-TiO_2 nanocomposites with different % of $Cu_{2-x}Se$. The Kubelka munk curves have been extrapolated to the x-ordinate to indicate the band gap values in eV.

Table S2. Atomic percentages ratio of the elements in the wide scan XPS spectrum of 1%$Cu_{2-x}Se$-TiO_2.

Element	Position	FWHM	Area	Aomic%
Ti 2p	459.03	2.53	447684.89	21.28
C 1s	285.03	3.49	33045.69	12.27
O 1s	530.03	2.84	476988.39	60.43
N 1s	400.03	3.26	6694.62	1.38
F 1s	689.03	3.01	39211.85	3.29
Se 3p	156.03	3.93	11876.51	0.97
Cu 2p	932.03	3.09	26099.72	0.38

a) b)

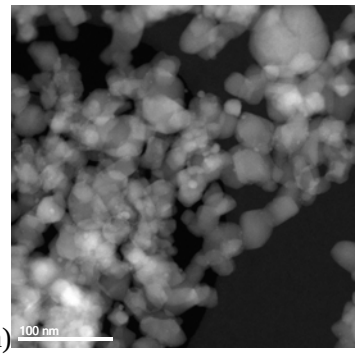

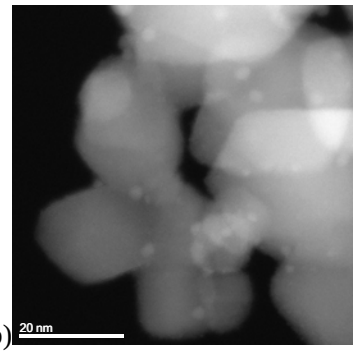

c)

Element	%Mass	%Atomic
O K	94.91	98.73
Cu K	3.91	1.02
Se K	1.18	0.25
Total	100.00	100.00

d)

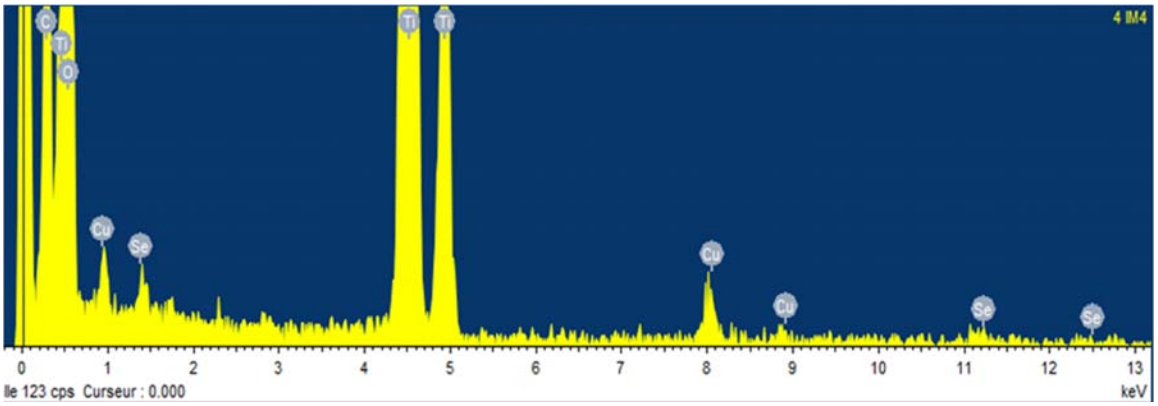

Figure S7. STEM images at different resolution of 1mol% $Cu_{2-x}Se$-TiO_2 nanocomposites (a & b), elemental composition of the sample as determined by EDXS analysis (since Ti grid was used, its analysis was not possible) (c), and EDX spectrum of this nanocomposites (Ti and C signals from substrate) (d).

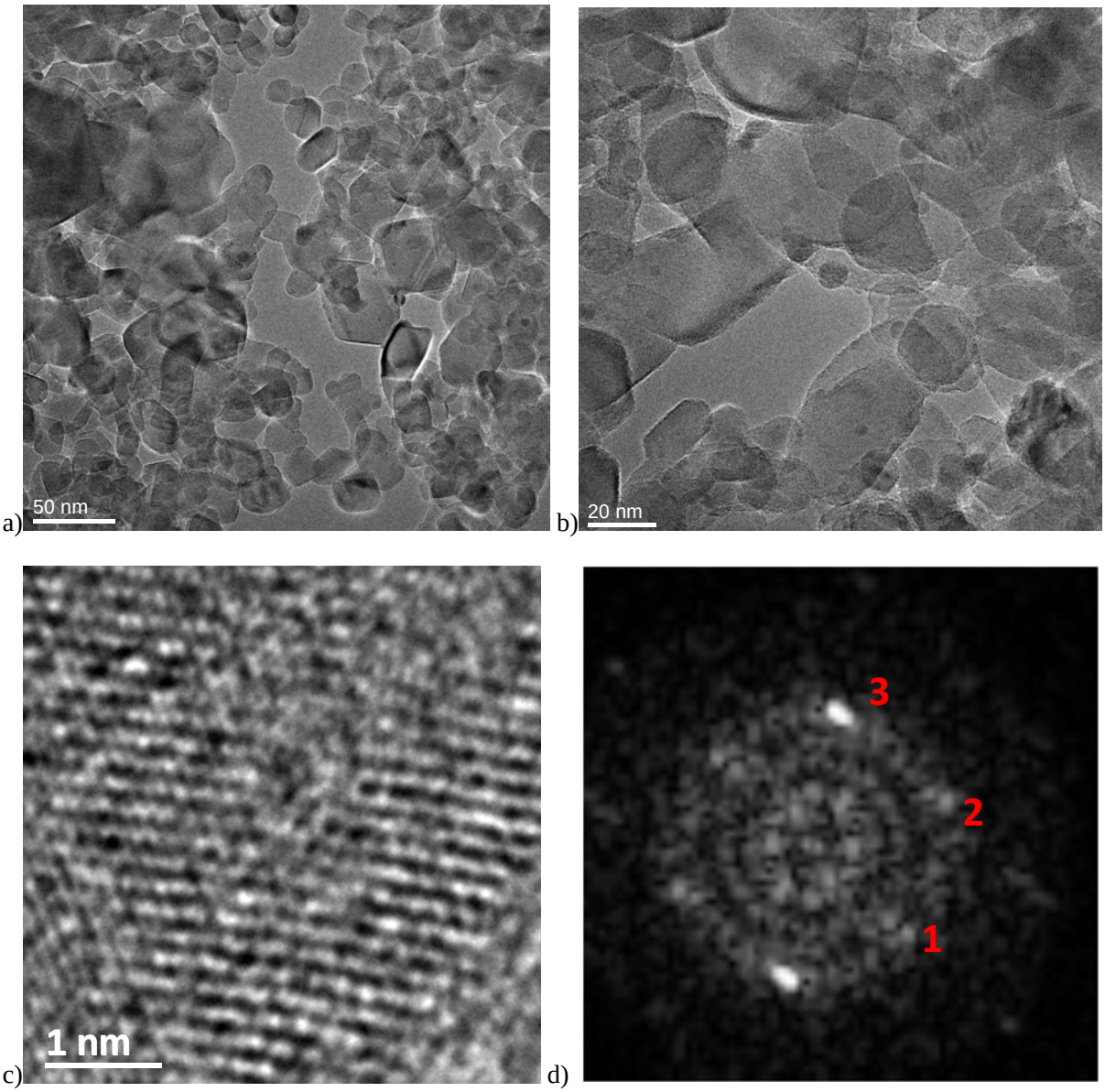

Spot n° :	h k l	d(exp.) nm	α(exp.)	d(théo.) nm	α(théo.)
1	2 2 0	0.2166	0.00	0.2070	0.00
2	0 2 2	0.1949	61.30	0.2070	60.00
3	-2 0 2	0.2091	121.95	0.2070	120.00

$Cu_{2-x}Se$ (03-065-7737)

Figure S8. TEM and HR-TEM images of 1% $Cu_{2-x}Se$-TiO_2 nanocomposite at different resolution (a-c) and selected area diffraction pattern of $Cu_{2-x}Se$ NPs (d).

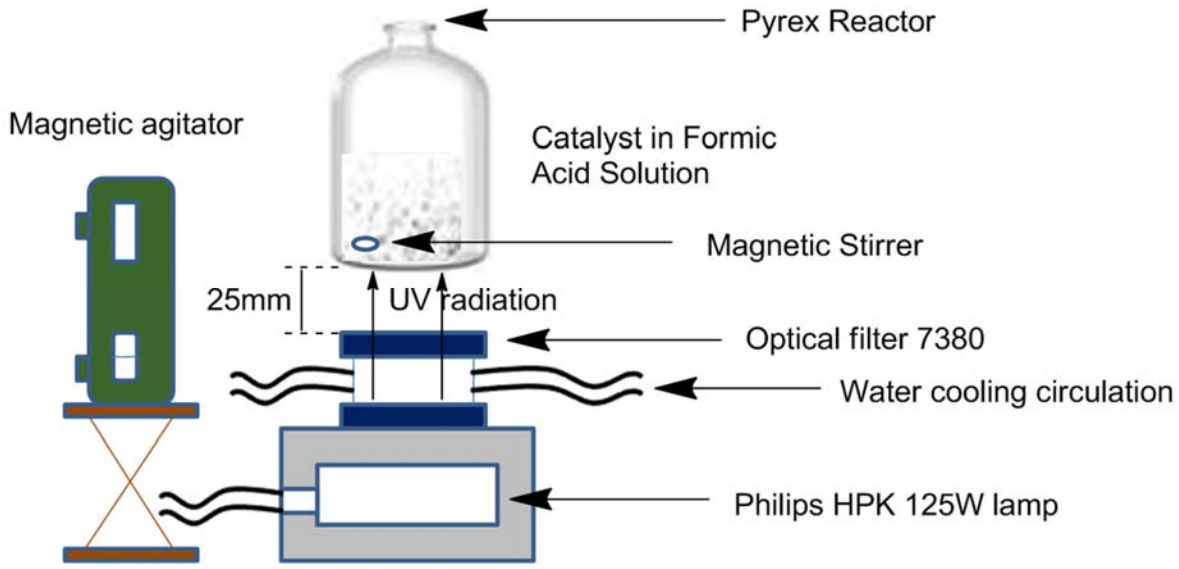

Figure S9. The experimental setup for FA photodegradation under UV light.

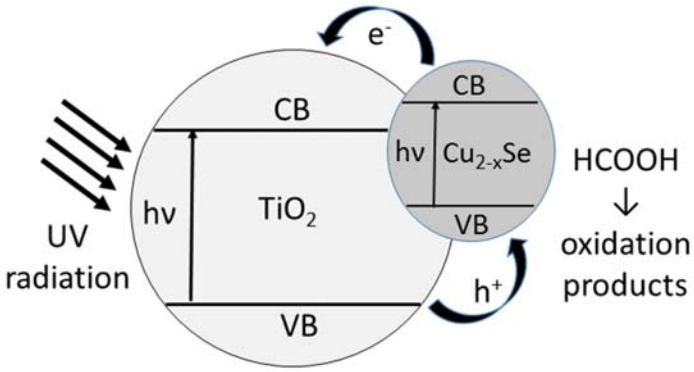

Figure S10. Schematic diagram of the charge-transfer processes between $Cu_{2-x}Se$ and TiO_2 during photodegradation of formic acid.

$$TiO_2 + h\nu \longrightarrow TiO_2(e^-) + TiO_2(h^+) \quad (S1)$$

$$Cu_{2-x}Se + h\nu \longrightarrow Cu_{2-x}Se(e^-) + Cu_{2-x}Se(h^+) \quad (S2)$$

$$e^- + O_2 \longrightarrow O_2^{\bullet -} \quad (S3)$$

$$h^+ + HCOOH \longrightarrow H^+ + HCOO^{\bullet} \quad (S4)$$

$$h^+ + HCOO^{\bullet} \longrightarrow CO_2 + H^+ \quad (S5)$$

$$H^+ + O_2^{\bullet -} \longrightarrow HO_2^{\bullet} \quad (S6)$$

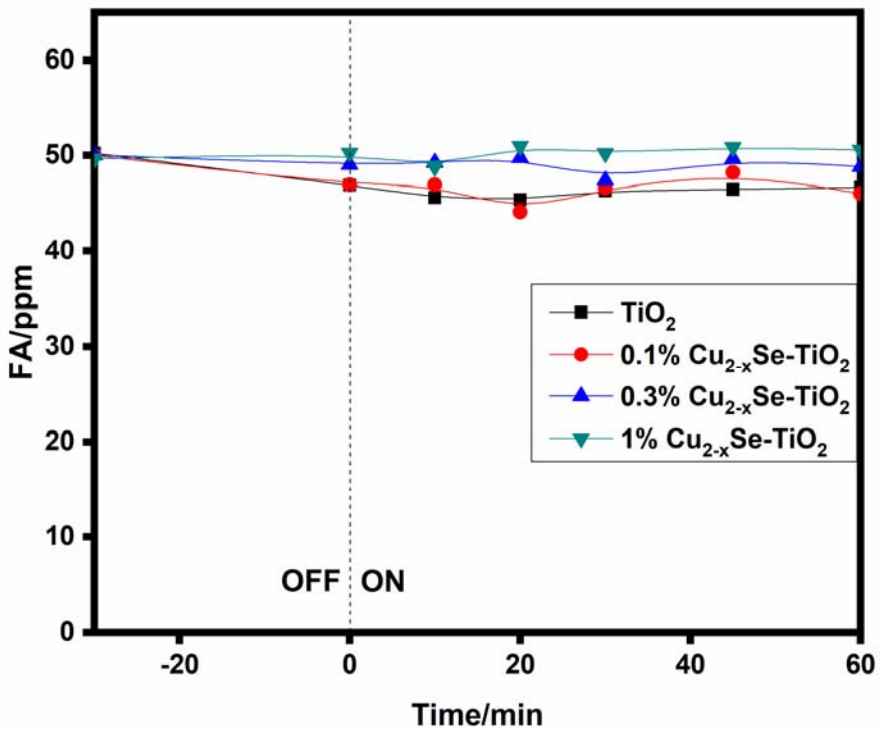

Figure S11. Photodegradation of FA by using TiO_2, and $Cu_{2-x}Se$-TiO_2 with different % of $Cu_{2-x}Se$ under visible light.

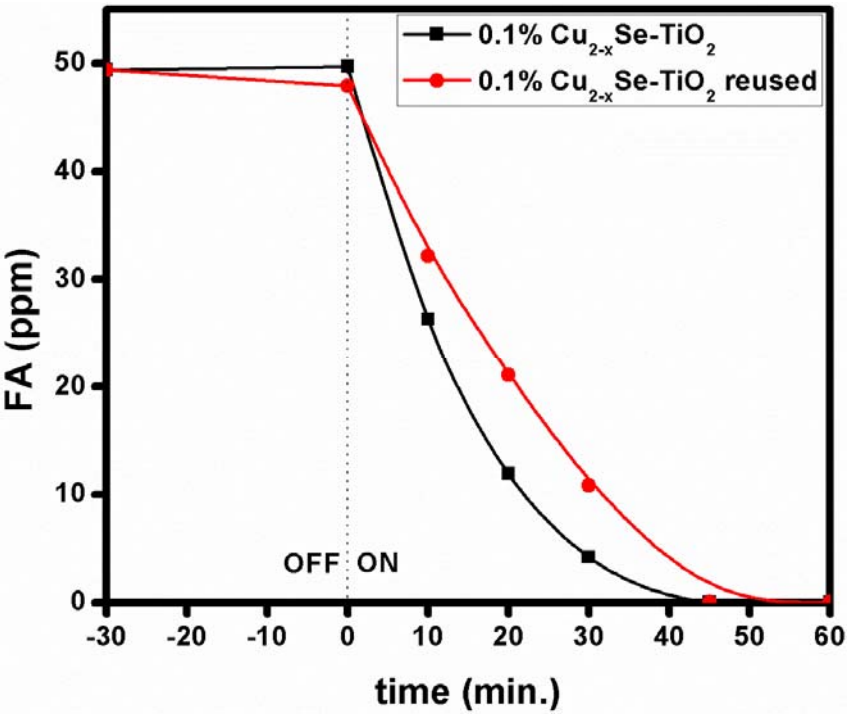

Figure S12. Photodegradation of FA using recycled catalyst.

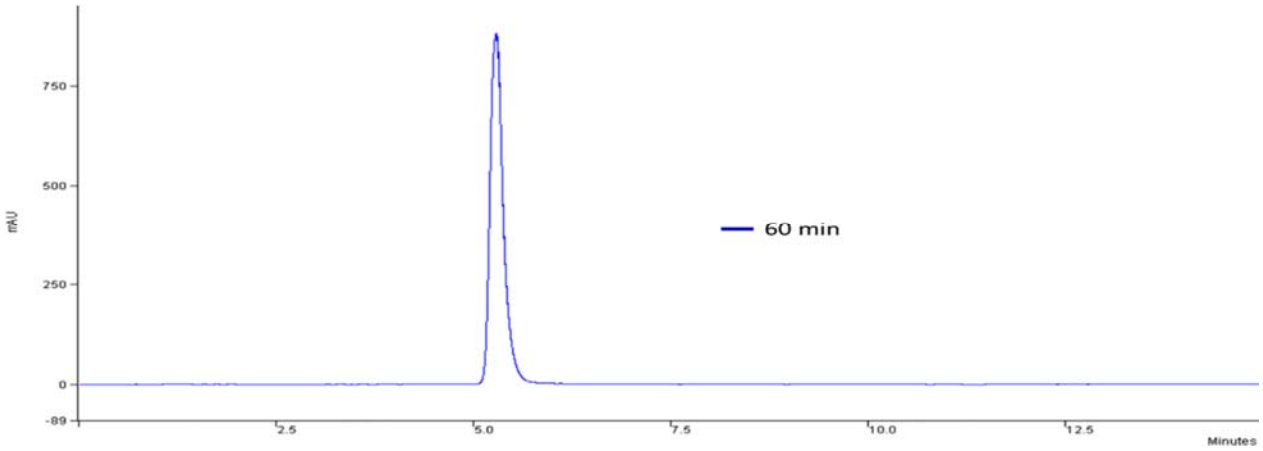

Figure S13. HPLC chromatogram for acidic water at 60 minutes with no extra peak corresponding to any organic molecule except the injection peak at 5.27 minutes. Other samples from HPLC results show similar chromatograms, thus conforming that these catalysts remain chemically stable during photocatalytic experiments.